ACCOUNTS of chemical research

pubs.acs.org/accounts Article

Manganese Carbonyl Complexes as Selective Electrocatalysts for CO_2 Reduction in Water and Organic Solvents

Published as part of the Accounts of Chemical Research special issue "CO2 Reductions via Photo and Electrochemical Processes".

Bhavin Siritanaratkul, Catherine Eagle, and Alexander J. Cowan*

Cite This: *Acc. Chem. Res.* 2022, 55, 955−965 Read Online

ACCESS | Metrics & More | Article Recommendations

CONSPECTUS: The electrochemical reduction of CO_2 provides a way to sustainably generate carbon-based fuels and feedstocks. Molecular CO_2 reduction electrocatalysts provide tunable reaction centers offering an approach to control the selectivity of catalysis. Manganese carbonyl complexes, based on $[Mn(bpy)(CO)_3Br]$ and its derivatives (bpy = 2,2′-bipyridine), are particularly interesting due to their ease of synthesis and the use of a first-row earth-abundant transition metal. $[Mn(bpy)(CO)_3Br]$ was first shown to be an active and selective catalyst for reducing CO_2 to CO in organic solvents in 2011. Since then, manganese carbonyl catalysts have been widely studied with numerous reports of their use as electrocatalysts and photocatalysts and studies of their mechanism.

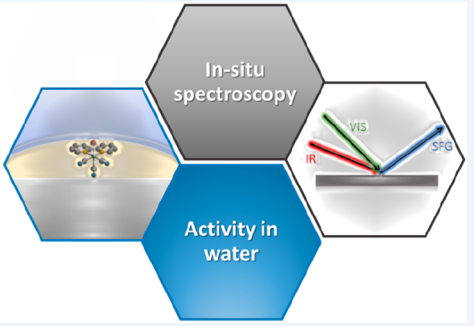

This class of Mn catalysts only shows CO_2 reduction activity with the addition of weak Brønsted acids. Perhaps surprisingly, early reports showed increased turnover frequencies as the acid strength is increased without a loss in selectivity toward CO evolution. It may have been expected that the competing hydrogen evolution reaction could have led to lower selectivity. Inspired by these works we began to explore if the catalyst would work in protic solvents, namely, water, and to explore the pH range over which it can operate. Here we describe the early studies from our laboratory that first demonstrated the use of manganese carbonyl complexes in water and then go on to discuss wider developments on the use of these catalysts in water, highlighting their potential as catalysts for use in aqueous CO_2 electrolyzers.

Key to the excellent selectivity of these catalysts in the presence of Brønsted acids is a proton-assisted CO_2 binding mechanism, where for the acids widely studied, lower pK_a values actually favor CO_2 binding over Mn−H formation, a precursor to H_2 evolution. Here we discuss the wider literature before focusing on our own contributions in validating this previously proposed mechanism through the use of vibrational sum frequency generation (VSFG) spectroelectrochemistry. This allowed us to study $[Mn(bpy)(CO)_3Br]$ while it is at, or near, the electrode surface, which provided a way to identify new catalytic intermediates and also confirm that proton-assisted CO_2 binding operates in both the "dimer" and primary (via $[Mn(bpy)(CO)_3]^-$) pathways. Understanding the mechanism of how these highly selective catalysts operate is important as we propose that the Mn complexes will be valuable models to guide the development of new proton/acid tolerant CO_2 reduction catalysts.

KEY REFERENCES

- Walsh, J. J.; Neri, G.; Smith, C. L.; Cowan, A. J. Electrocatalytic CO2 reduction with a membrane supported manganese catalyst in aqueous solution. *Chem. Commun.* **2014**, *50*, 12698−12701.[1] *This work used a simple approach to immobilize the Mn complex on a carbon support allowing for its study in aqueous solvent for the first time, demonstrating that CO_2 reduction selectivity was retained.*
- Walsh, J. J.; Neri, G.; Smith, C. L.; Cowan, A. J. Water-Soluble Manganese Complex for Selective Electrocatalytic CO2 Reduction to CO. *Organometallics* **2019**, *38*, 1224−1229.[2] *Here we showed the activity and selectivity of a carboxylic acid derivative in water across a wide pH range.*
- Neri, G.; Walsh, J. J.; Teobaldi, G.; Donaldson, P. M.; Cowan, A. J. Detection of catalytic intermediates at an electrode surface during carbon dioxide reduction by an earth-abundant catalyst. *Nature Catalysis* **2018**, *1*, 952−

Received: November 5, 2021
Published: March 14, 2022

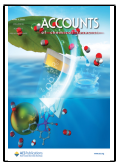

https://doi.org/10.1021/acs.accounts.1c00692
Acc. Chem. Res. 2022, 55, 955−965

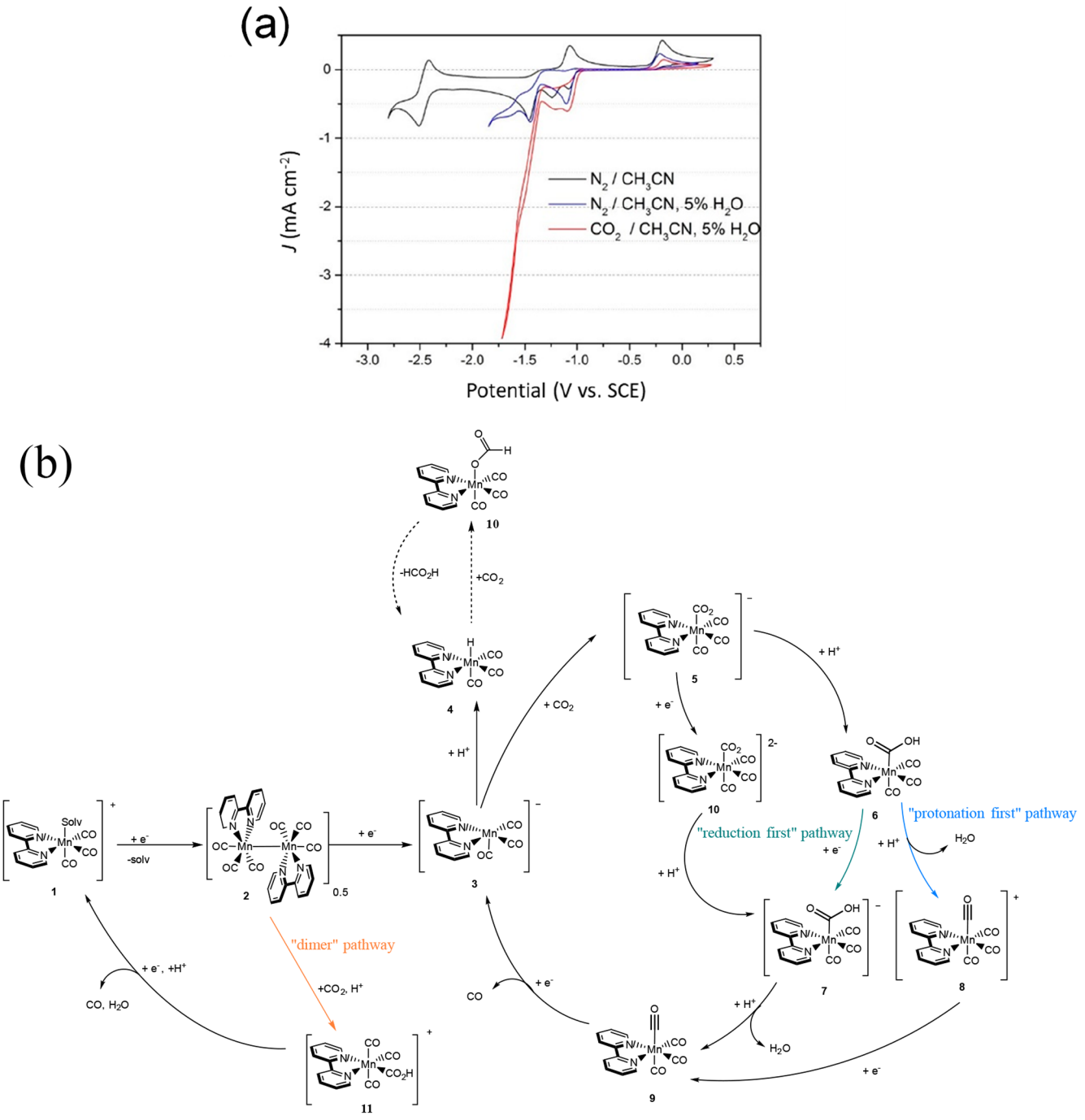

Figure 1. (a) CV of [Mn(bpy)(CO)$_3$Br] in CH$_3$CN at a glassy carbon electrode under the conditions indicated. (b) Proposed catalytic cycle of [Mn(bpy)(CO)$_3$Br]. Three main pathways for CO_2 reduction to CO have been evidenced through a wide range of spectroscopic, electrochemical, and theoretical studies.[22] These are the dimer pathway (orange), protonation first pathway (blue), and reduction first pathway (green). An additional proposed pathway to form formate or formic acid is also shown[28] (dashed lines). Panel b adapted from ref 3 with permission from Springer Nature.

959.[3] *This study used vibrational sum-frequency generation spectroscopy to follow the reaction mechanisms of the Mn catalyst transiently at an electrode during carbon dioxide reduction.*

- Neri, G.; Donaldson, P. M.; Cowan, A. J. In situ study of the low overpotential "dimer pathway" for electrocatalytic carbon dioxide reduction by manganese carbonyl complexes. *Phys. Chem. Chem. Phys.*, **2019**, *21*, 7389−7397.[4] *Here we examined the surface behavior of the Mn catalyst as it arrives at the electrode and also explored the mechanism of the less studied lower overpotential reaction pathway.*

1. INTRODUCTION

Electrochemical CO_2 reduction will be needed to enable a circular carbon economy and it is proposed to play an important role in managing CO_2 emissions.[5−7] Electrochemical CO_2 conversion at scale is expected to make use of point

https://doi.org/10.1021/acs.accounts.1c00692
Acc. Chem. Res. 2022, 55, 955−965

sources of CO_2, such as flue gas from heavy industries. Metal electrodes and metallic electrocatalysts[8] deposited onto high surface area supports have demonstrated that reduction of pure CO_2 feeds can achieve high current densities (up to 1 A cm^{-2}) in CO_2 electrolyzers.[9] However, as the CO_2 concentration is decreased and impurities such as O_2, NO_x, and SO_x, are added to simulate a typical flue gas stream, changes in selectivity have been reported.[10,11] Molecular catalysts[12−15] provide an opportunity to achieve desired reactant and product selectivity by altering the ligands surrounding the metal center to tune the reaction center's electronics and steric bulk. Therefore, they are particularly interesting as both models of how CO_2 selectivity can be controlled and potential practical-scale catalysts for application in an immobilized configuration.

A widely studied class of molecular electrocatalysts is those based on [*fac*-Re(bpy)$(CO)_3$Cl] (bpy = 2,2′-bipyridine, hereafter the *fac*- is assumed for all tricarbonyl structures unless otherwise stated). This catalyst was first reported in the 1980s to produce CO both photocatalytically and electrochemically from CO_2, displaying high Faradaic efficiencies for CO and good stability under electrocatalytic conditions.[16,17] Despite these promising results, Re has low natural abundance.[18] Early on, [Mn(bpy)$(CO)_3$Br] was examined as a possible alternative high-abundance catalyst, but initial reports in organic solvents noted a lack of activity toward CO_2.[19] It was not until 2011 in a breakthrough study by Deronzier and co-workers[20] that [Mn(bpy-R)$(CO)_3$Br] (R = H or alkyl group at the 4,4′ position) was shown to be an active electrocatalyst for CO_2 reduction in organic solvents, but only when a Brønsted acid was added. A typical cyclic voltammogram of [Mn(bpy)$(CO)_3$Br] in acetonitrile, similar to that measured in those first reports, is shown in Figure 1a, and a proposed catalytic cycle is shown in Figure 1b. Under N_2, initial reduction at −1.2 V_{SCE} results in the loss of Br^- and then dimerization to form $[Mn(bpy)(CO)_3]_2$. This dimer complex is reduced at −1.5 V_{SCE} to form the main catalytically active species $[Mn(bpy)(CO)_3]^-$ as indicated by the large increase in current under CO_2 and in the presence of a proton source. In competition with CO evolution is H_2 production, which occurs via the formation of [Mn(bpy)$(CO)_3$H].

The initial study by Deronzier and colleagues[20] led to a large number of follow-on works on this class of catalyst, of which several reviews exist.[13,21−24] In this Account, we discuss one of the most interesting aspects, the need for a Brønsted acid for any measurable CO_2 reduction to occur.[16,17] This finding was confirmed in a study by the Kubiak group in 2013, on a derivative, [Mn(bpy(^{t}Bu)$_2$)$(CO)_3$Br], in acetonitrile with the addition of the weak acids water, methanol, and 2,2,2-trifluoroethanol (TFE), where higher turnover frequencies were achieved than with the parent complex.[25] Also, the turnover frequency of the Mn catalyst was shown to increase with acid strength, and in general with higher concentrations of acid, without a loss in selectivity toward CO_2 reduction. These experiments on the complex in aprotic solvents with an acid source led us to ask in 2014,[1] could the performance of [Mn(bpy)$(CO)_3$Br] be further improved by use in a protic solvent, in particular water?

Developing CO_2 reduction catalysts that are selective in water is important; in a practical electrolyzer, the CO_2 reduction reaction will need to be coupled to a sustainable oxidation reaction, presumably water oxidation. In particular, there is current interest in understanding how to develop systems that can selectively reduce CO_2 in an acidic environment[26] as operating CO_2 electrolyzers at high pH leads to carbonate formation with consequential decreased CO_2 conversion efficiencies.[27] With conventional metal catalysts (e.g., Ag, Au, or Cu) operating at low pH is challenging due to competitive hydrogen evolution as a result of the high proton concentration. Therefore, the development and mechanistic study of molecular electrocatalysts that show high selectivity to CO_2 reduction in the presence of high proton concentrations is of great interest to the field. Here we describe in section 2 the use of this class of Mn catalysts for CO_2 reduction in water, focusing on early work from our own laboratory before discussing wider developments in the field. In section 3, we discuss mechanistic studies on the role of the acid source in the CO_2 reduction mechanism in an effort to understand how these catalysts achieve selectivity. In particular, we introduce the use of vibrational sum frequency generation (VSFG) spectroscopy, which confirmed a previously proposed proton-assisted CO_2 binding mechanism for the main catalytic pathways, rationalizing why these catalysts can operate even in proton-rich environments.

2. [Mn(bpy)$(CO)_3$Br] AND ITS DERIVATIVES AS CO_2 REDUCTION CATALYSTS IN WATER

To test how [Mn(bpy)$(CO)_3$Br] behaved in the presence of aqueous electrolytes, we initially applied a simple approach previously described for a range of catalysts including [Re(bpy)$(CO)_3$Br],[29] where we deposited the Mn complex directly onto a glassy carbon electrode (GCE) using a Nafion ionomer support.[1] Direct study of the mechanism of the catalyst within the Nafion membrane is challenging but CVs indicated that despite being immobilized and used at pH 7, the catalyst showed very similar behavior to that observed when it is dissolved in aprotic solvents with the largest current enhancement under CO_2 occurring following the formation of $[Mn(bpy)(CO)_3]^-$. Intriguingly in the Nafion membrane, dimerization is believed to still occur following initial reduction of [Mn(bpy)$(CO)_3$Br], prior to the formation of the active $[Mn(bpy)(CO)_3]^-$ catalyst, as indicated by the oxidation peak of $[Mn_2(bpy)_2(CO)_6]$. A linear dependence of peak current with scan rate for the reduction of [Mn(bpy)$(CO)_3$Br] indicated that the complex was not solubilized in the polymer, and no evidence of Mn loss into the electrolyte was found suggesting that dimer formation was the result of electroactive aggregates; however definitive evidence of the mechanism of dimerization within Nafion is still missing. Regardless of the possible mechanisms of dimerization the most important outcome of this first study was that once formed $[Mn(bpy)(CO)_3]^-$ displayed good selectivity for CO_2 reduction in water at pH 7 with a CO/H_2 ratio of 2:1 being achieved at −1.4 $V_{Ag/AgCl}$ and TON of up to 470. This demonstrated the viability of using this complex in protic solvents and indicates that CO_2 reduction selectivities on par with those seen in aprotic solvents could be achieved.

In the first studies of GCE/[Mn(bpy)$(CO)_3$Br]/Nafion electrodes, current densities were low (0.3 mA cm^{-2}) due to the majority of the catalyst present being electro-inactive. The addition of multiwalled carbon nanotubes (MWCNTs), increasing the electroactive content, led to a large increase in current density under CO_2 (up to 3 mA cm^{-2}, Figure 2), albeit with a partial loss in CO/H_2 selectivity (dropping to ∼1:2).[1] A subsequent study investigated a wider range of Mn complexes that contained modifications to the 4,4′ positions of the 2,2′-bipyridine ligand immobilized in a similar manner with

https://doi.org/10.1021/acs.accounts.1c00692
Acc. Chem. Res. 2022, 55, 955−965

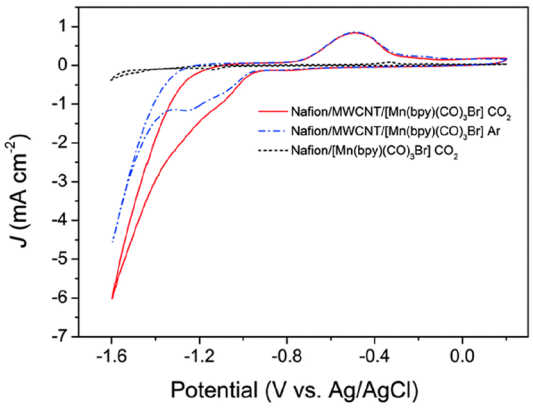

Figure 2. Cyclic voltammetry of $[Mn(bpy)(CO)_3Br]$ immobilized in a Nafion film on a glassy carbon electrode in 30 mM phosphate buffer, pH ∼7, showing the current enhancement from MWCNT addition. Reproduced from ref 1 with permission from the Royal Society of Chemistry.

MWCNTs.[30] Among the complexes studied $[Mn(bpy(^tBu)_2)(CO)_3Br]$, which was first reported by Kubiak and colleagues,[25] gave the highest level of selectivity toward CO ($CO/H_2 \approx 1$); however the CO partial current density was lower than the original unmodified bipyridine complex. Also studied were $[Mn(bpy(OH)_2)(CO)_3Br]$ and $[Mn(bpy(COOH)_2)(CO)_3Br]$, but both complexes gave disappointing levels of selectivity when immobilized, with $CO/H_2 \approx 0.28$ and 0.33, respectively.[30] The initial studies of the Mn catalysts deposited on GCE made use of the low solubility of $[Mn(bpy)(CO)_3Br]$ in water;[1,30] however relatively low electroactive contents were achieved, and the current densities reported above are ∼30 times lower than is required for application in a practical electrolyzer (>100 mA cm^{-2}).

Subsequent studies have reported more advanced approaches to immobilize manganese carbonyl catalysts with several achieving notably higher current densities. Reisner and colleagues developed a derivative where the catalyst was anchored to carbon nanotubes through a pyrene-modified

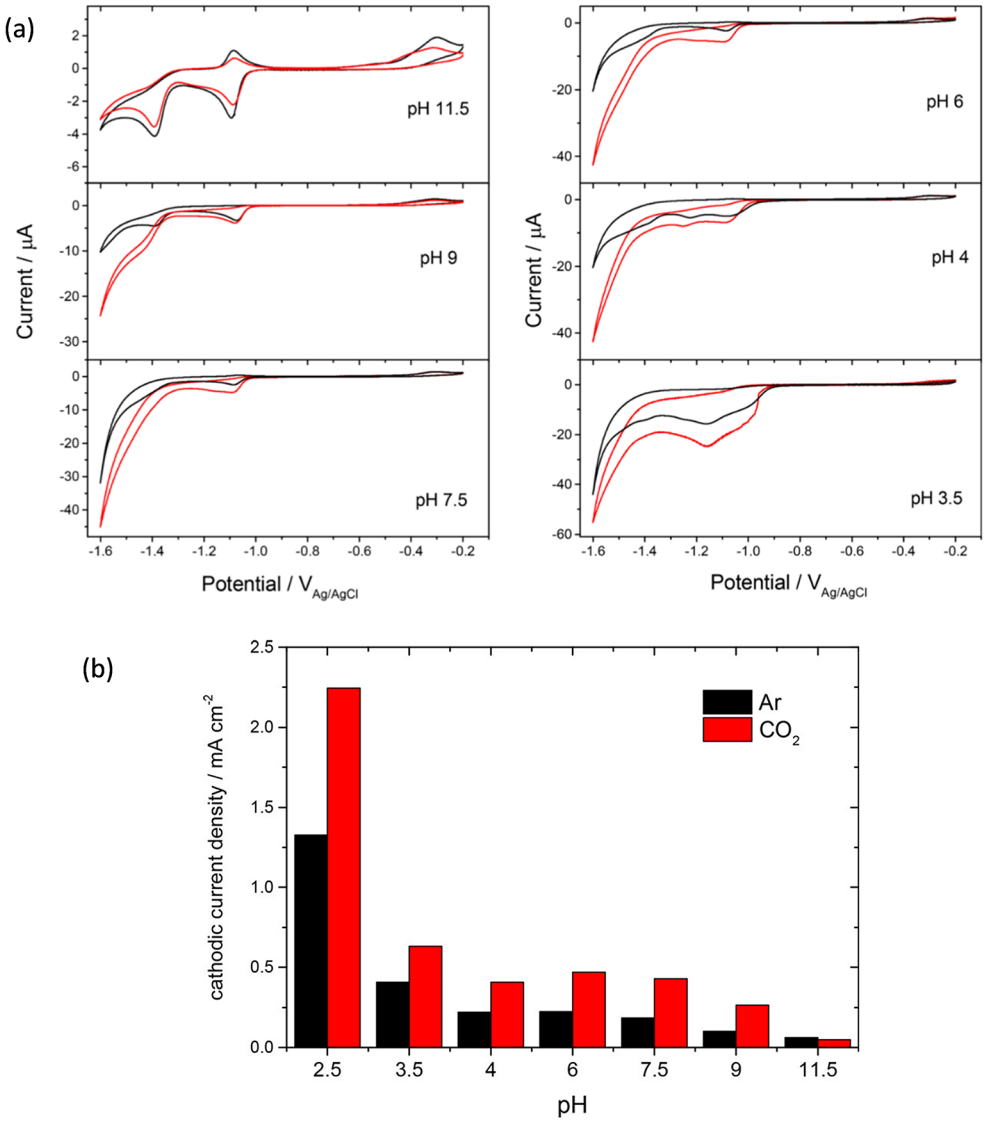

Figure 3. $[Mn^I(bpy)(COOH)_2)(CO)_3Br]$ is a water-soluble CO_2 reduction catalyst that shows good selectivity toward CO production at pH 9. CVs are shown at a range of pH values under Ar (black) and under CO_2 (red), recorded at 100 mV s^{-1} (a), current at −1.5 $V_{Ag/AgCl}$ vs pH under argon (black) and CO_2 (red) (b). Reproduced with permission from ref 2. Copyright 2019 American Chemical Society.

https://doi.org/10.1021/acs.accounts.1c00692
Acc. Chem. Res. 2022, 55, 955−965

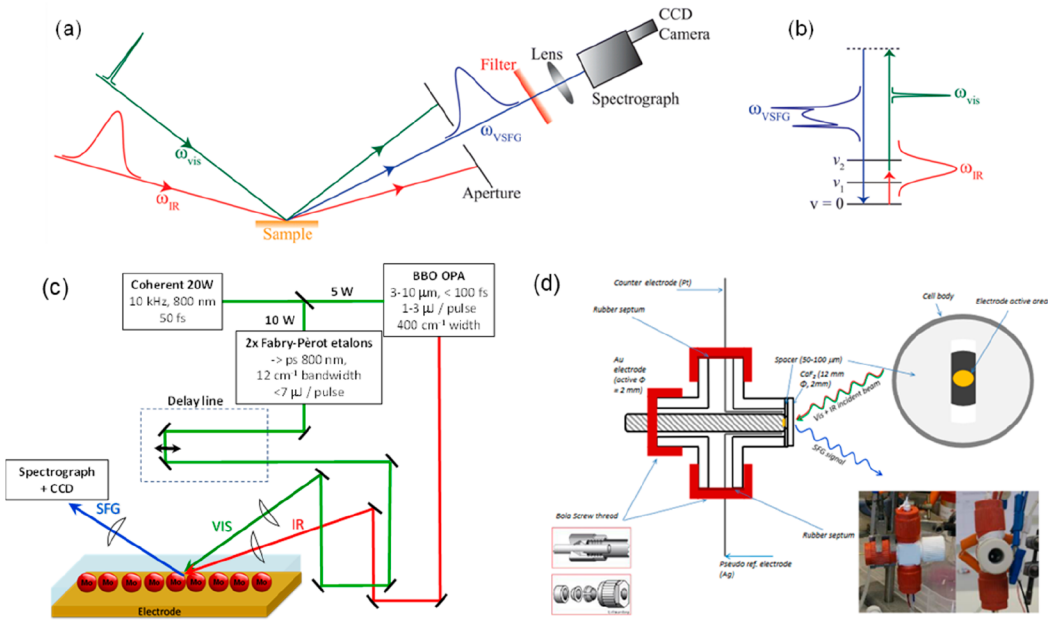

Figure 4. (a,b) Broad-band (<150 fs) mIR VSFG experiments. The data shown here uses a broad-band setup where a broad-band mIR pulse is incident on the electrode surface and overlapped with a narrow-band (>1 ps) visible laser pulse. (c) Experimental setup used in the VSFG data in refs 3, 4, and 40 at the UK Central Laser Facility and (d) SEC cell for VSFG with thin path-length. Panels a and b reproduced from ref 41 with permission from the PCCP Owner Societies. Panel d reproduced with permission from ref 40. Copyright 2017 American Chemical Society.

bipyridine ligand, which was found to show a stable current density of 0.5 mA cm^{-2} (−1.1 V_{SHE}) with a good selectivity for CO production (maximum Faradaic efficiency of 34%) at pH 7.4.[28] Interestingly this system also produced appreciable concentrations of formate, which is not a common observation in other electrocatalytic studies in water described below. Excellent selectivity for CO production (>80% Faradaic efficiency) and a stable current density of 5 mA cm^{-2} were reported from a polymerized manganese carbonyl complex on MWCNTs in a pH 7 electrolyte when K^+ ions were present at high concentrations.[31] Of great relevance is also the work of Vizza and co-workers who prepared [Mn(apbpy)$(CO)_3$Br] (apbpy = 4-(4-aminophenyl)-2,2′-bipyridine), which can be electrochemically grafted onto carbon cloth.[32] In this way, electrodes with the catalytic center covalently bound onto the support can be prepared and achieved Faradaic efficiencies of ∼60% for CO production at −1.4 $V_{Ag/AgCl}$ in CO_2 saturated $KHCO_3$. Very recently, studies of this catalyst bound onto a gas diffusion electrode showed that the mass normalized turnover frequencies of the catalyst exceeded those of a benchmark Au catalyst.[33] Another strategy to achieve higher electroactive concentrations of catalytic centers, and therefore potentially higher current densities, is to incorporate the Mn catalytic center directly within a high surface area porous framework. Examples that use a Mn catalytic center for CO_2 reduction in water include a conjugated microporous polymer[34] and a covalent organic framework[35] with the latter achieving an impressive CO partial current density of 11 mA cm^{-2} and selectivity (55% Faradaic efficiency) at pH 7.4.[33]

The examples of [Mn(bpy)$(CO)_3$Br] derivatives immobilized onto and into electrode supports for CO_2 reduction in water have demonstrated that a good level of selectivity (typically ≥1:1 CO/H_2) can be achieved at pH ∼7. However, it is difficult to quantify the intrinsic selectivity of the catalyst due to the possibility of hydrogen being evolved from the carbon support or impurities within. In order to better understand the behavior of the Mn catalyst in a wide pH range, we also developed a water-soluble Mn diimine CO_2 reduction complex [Mn(bpy$(COOH)_2$)$(CO)_3$Br], where bpy$(COOH)_2$ = 4,4′-dicarboxy-2,2′-bipyridine. The solubility of the catalyst allowed for experiments using a Hg amalgam electrode, which has a high overpotential for hydrogen evolution making it ideal for analytical electrochemistry in water at a range of pH values.[2] UV/vis spectroscopy showed a pH dependence due to the changing protonation state of the carboxylate groups and also indicated that the bromide ligand was readily displaced by water at open circuit. In contrast to the equivalent Re complex[36] where the displacement of the aqua ligand by bicarbonate led to a loss in solubility at some pH values under CO_2, the Mn analogue retained solubility under CO_2, and no evidence of carbonate/bicarbonate ligation was observed.[12] CVs of $[Mn^{I}(bpy(COO)_2)(CO)_3]^-$ under Ar and CO_2 at a range of pH values were similar to other complexes from this class in conventional organic solvents with an initial reduction between −1.0 and −1.1 $V_{Ag/AgCl}$, depending upon pH, leading to loss of a solvent ligand and dimer formation, and a further reduction between −1.4 and −1.3 $V_{Ag/AgCl}$ formed the active $[Mn(bpy(COO)_2)(CO)_3]^{3-}$ (Figure 3a). At the highest pH values studied (>9), minimal CO_2 reduction occurs, presumably due to a combination of low concentrations of available CO_2 and H^+. Bulk electrolysis was only carried out at a single pH in this initial communication but notably between pH 9 and 2.5 a large enhancement in catalytic current occurred under CO_2 with the greatest increases in current under CO_2 occurring at the lowest pH values (Figure 3b). This indication of CO_2 catalysis even at the lowest pH values studied is of particular interest because at pH < 4 bicarbonate formation is no longer a significant process; therefore the development and study of catalysts that can operate selectively toward CO_2 reduction under these conditions may provide a way to enable acid CO_2 electrolyzers.[26]

https://doi.org/10.1021/acs.accounts.1c00692
Acc. Chem. Res. 2022, 55, 955−965

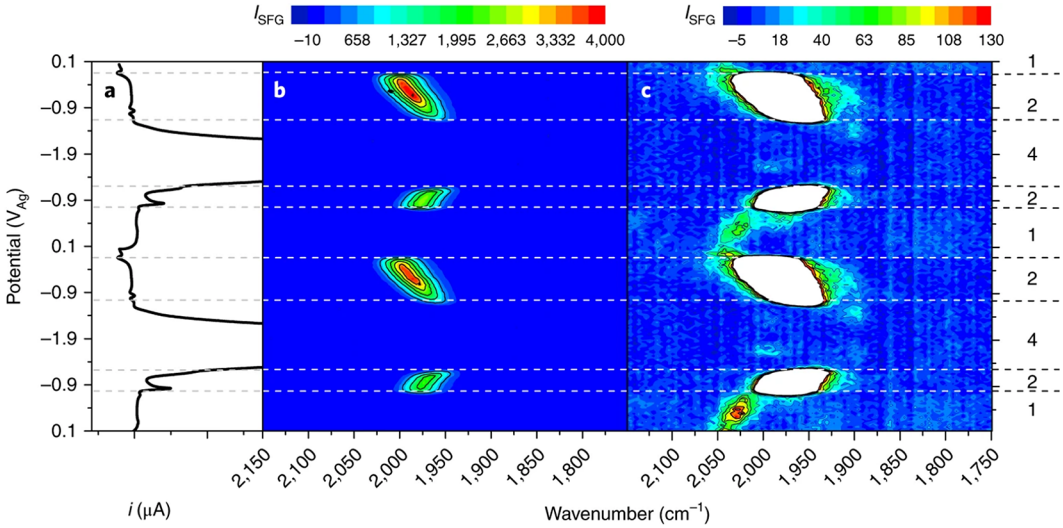

Figure 5. CV (a) of $[Mn(bpy)(CO)_3Br]$ in CH_3CN in the presence of 1.5 M TFE under Ar and VSFG spectra (b, c) recorded in situ of the complex at the working electrode. Panel c is an expansion (*z*-axis, VSFG intensity) of panel b. The numbers on the right correspond to the spectral assignments. (1) $[Mn(bpy)(CO)_3(solv)]^+$; (2) $[Mn_2bpy_2(CO)_6]$; (4) $[Mn(bpy)(CO_3)H]$. Adapted from ref 3 with permission from Springer Nature.

3. MECHANISTIC STUDIES ON $[Mn(bpy)(CO)_3Br]$ AT ELECTRODE SURFACES: UNDERSTANDING THE ROLE OF THE BRØNSTED ACID TO RATIONALIZE THE SELECTIVITY TOWARD CO_2

The electrochemical behavior of $[Mn(bpy)(CO)_3Br]$ has been studied in detail using a wide range of spectroscopic techniques. Covering these in detail is not the aim of this Account, and a more comprehensive review is provided by Grills et al.[22] Instead we focus on attempts to understand how these Mn catalysts retain selectivity for CO_2 reduction to CO in protic environments. As noted in section 1, two key studies were the original work of Deronzier and colleagues who noted the need for an acid source for catalysis to occur[20] and work from the Kubiak group on the behavior of $[Mn(bpy(^tBu)_2)(CO)_3Br]$ with a range of acids.[25] In Kubiak's 2013 study, it was proposed that the Brønsted acid was required to protonate the initially formed CO_2 adduct, with protonation either stabilizing the $Mn-CO_2$ species or facilitating the cleavage of a C−O bond. DFT calculations following on from this work by Carter and colleagues confirmed that without an acid present CO_2 binding was endergonic.[37,38] But once phenol was added, the process became exergonic, and initial CO_2 binding was followed by the barrierless, strongly exergonic protonation of the $Mn-CO_2$ adduct.[37,38] This finding has since been further validated and expanded upon in DFT calculations where TFE is the acid source, which showed a dual role for the acid, stabilizing the $Mn-CO_2$ adduct with subsequent rapid protonation and exergonic carbonation of the conjugate base providing additional driving force for the overall generation of a $Mn-CO_2H$ intermediate.[39] The DFT studies of the Carter group also represented the first report of the presence of two catalytic pathways for CO evolution following proton assisted CO_2 binding to $[Mn(bpy)(CO)_3]^-$, labeled the "protonation first" and "reduction first" pathways in Figure 1b. These calculations provided a rationale for the excellent selectivity and improved turnover frequency in the presence of stronger acids, and a framework by which we can understand the selectivity of the catalysts in water. However, direct detection of many of the short-lived intermediates proposed has historically been a challenge with conventional spectroscopies where the need to electrochemically generate high concentrations of species in the bulk inevitably makes the detection of short-lived transient species at the electrode surface difficult.

Our own contribution has focused on using vibrational sum frequency generation (VSFG) spectroscopy to study Mn catalysts at the electrode surface in the presence of a range of acids, with the aim of validating the calculated role of the Brønsted acid in CO_2 reduction. In a VSFG experiment, two incident, short laser pulses are overlapped on the sample interface (in this case the working electrode surface), and the light is generated at the sum of the frequency of the two input pulses (Figure 4a,b). In our experiments, we use a broad-band (typically 500 cm^{-1} fwhm, 50 fs) tunable mid-infrared (mIR) laser and a fixed wavelength visible (800 nm) laser that has a picosecond pulse duration and a time asymmetric shape. Both of these are transmitted through a thin-layer of electrolyte to the electrode surface (Figure 4c,d; for full details of the experimental apparatus, see ref 40). When the mIR laser frequency is resonant with a sum-frequency active vibrational mode, the VSFG light intensity is significantly increased and a vibrational spectrum of the species can be recorded. VSFG is often described as surface selective because signals are only generated in a non-centrosymmetric environment under the electric dipole approximation.[41,42] However, it is important to note that across the electrical double layer structure ordering can occur giving rise to VSFG signals and contributions from third order nonlinear polarization terms can also arise from molecules throughout the double layer; therefore this statement is not strictly correct.[43,44] Nonetheless VSFG spectroscopy provides a powerful way to study molecular electrocatalysts while they are near (within the double layer structure) or at the electrode surface, as sufficient ordering can occur due to the large electric fields present and the use of catalysts with nonzero dipole moments. A detailed review on the application of the technique to molecular electrocatalysts, which describes in more detail the experimental considerations and the route by which spectra are assigned and fitted, is available.[41]

https://doi.org/10.1021/acs.accounts.1c00692
Acc. Chem. Res. 2022, 55, 955−965

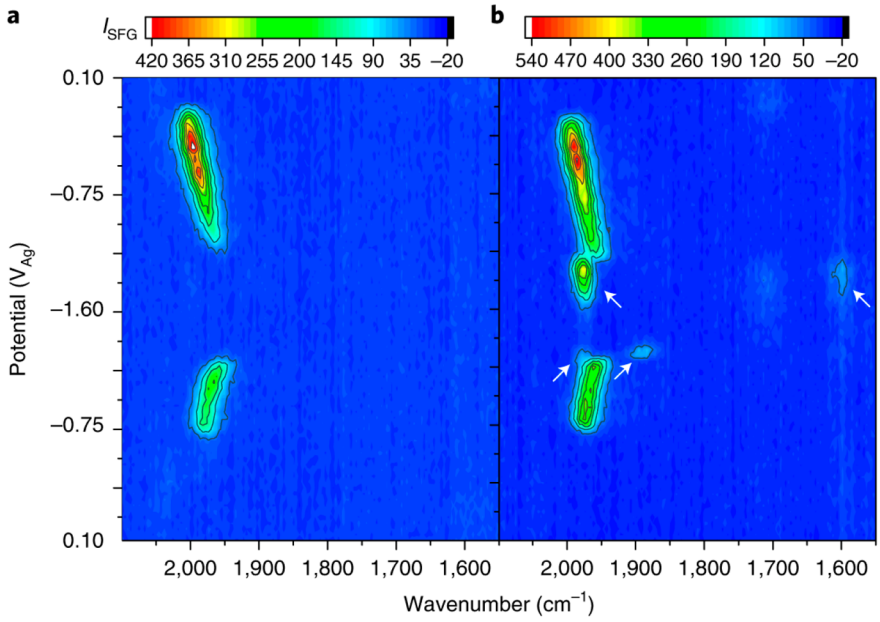

Figure 6. VSFG spectra of $[Mn(bpy)(CO)_3Br]$ in CH_3CN in the presence of 1.5 M TFE under Ar (a) and CO_2 (b). New CO_2 reduction intermediates at the electrode surface are indicated with white arrows with the bands at ∼1976 and ∼1600 cm^{-1} due to $[Mn(bpy)(CO)_4]^+$ and a band at ∼1875 cm^{-1} possibly due to $[Mn(bpy)(CO_2H)]^-$. Reproduced from ref 3 with permission from Springer Nature.

Initially we have carried out experiments in acetonitrile with added Brønsted acids as the need for IR transmission through the electrolyte prevents the study of aqueous electrolytes. VSFG data recorded during a CV of $[Mn(bpy)(CO)_3Br]$ in CH_3CN with TFE using a static Hg/Au amalgam electrode under an Ar atmosphere is shown in Figure 5.[3] In the VSFG experiments, we focus on the metal carbonyl stretching modes as they act as excellent reporter groups on the state of the metal center and prior bulk SEC-FTIR studies[1,45−47] provide a way to assign known species at the electrode surface. At open circuit, no ν(CO) bands were observed, but as the potential of the electrode was swept reductively from +0.1 V to −0.4 V (all potentials in the VSFG experiments in this section are versus a Ag pseudoreference electrode), a strong (∼2043 cm^{-1}) ν(CO) band increased in intensity (Figure 5c). A second broad, much weaker band around ∼1960−1940 cm^{-1} could also be observed upon careful inspection of individual spectra (not shown here) with both bands assigned to $[Mn(bpy)(CO)_3(CH_3CN)]^+$ (the solvent can displace the bromide ligand). The ν(CO) bands shifted in frequency with applied potential, giving a Stark shift of ∼35 cm^{-1} V^{-1}, demonstrating that the vibrational spectra were occurring from $[Mn(bpy)(CO)_3(CH_3CN)]^+$ experiencing a large electric field, which therefore must be at or near the electrode surface.

As expected from the past FTIR reports,[25,48] the reduction of $[Mn(bpy)(CO)_3(CH_3CN)]^+$ leads to formation of $[Mn_2(bpy)_2(CO)_6]$ (species 2, Figure 1b), and this in turn could be reduced at potentials negative of −0.9 V_{Ag}. The I_{SFG} of the ∼1970 cm^{-1} resonant mode of $[Mn_2(bpy)_2(CO)_6]$ is very intense (Figure 5b) as the visible laser pulse is resonant with an electronic transition of this complex.[20] We were unable to observe the anticipated active catalyst, $[Mn(bpy)(CO)_3]^-$, at the electrode surface. Instead, $[Mn(bpy)(CO)_3H]$ formed rapidly (Figure 5) in the absence of CO_2. Using VSFG spectroscopy, we found, in both the absence of a deliberately added acid and the presence of a number of acids (methanol, TFE, phenol), at the electrode surface $[Mn(bpy)(CO)_3H]$ formation in the absence of CO_2.[3,49] It is clear that at the electrode surface $[Mn(bpy)(CO)_3H]$ formation occurs very rapidly even in the absence of a deliberately added Brønsted acid (trace water is likely present), and the cause of the high selectivity of this complex toward CO_2 is not the lack of hydride formation. This is an interesting observation as FTIR spectroelectrochemistry had monitored the formation of $[Mn(6,6'$-dimesityl-2,2′-bipyridine$)(CO)_3]^-$ in the bulk electrolyte indicating its stability[50] and DFT calculations[38,39] predicted a ∼13−15 kcal mol^{-1} barrier to binding of H^+ to $[Mn(bpy)(CO)_3]^-$. One possible rationale of the VSFG result may be the presence of the large electric field at the electrode interface, which can have a profound effect on the relative stability of the species,[51] or due to preferential orientation/accumulation of protons at the electrode surface, with both situations highlighting the need to monitor the surface species.

Under CO_2 with TFE present, in the potential region where CO_2 reduction begins, $[Mn(bpy)(CO)_3H]$ is not detected; instead several new ν(CO) bands due to CO_2 reduction intermediates appear, Figure 6.[3] The intensity of the VSFG bands of the CO_2 reduction intermediates was greatest with acids with low pK_a values. Under CO_2 with the weakest acid studied (e.g., methanol), and when no acid was present, VSFG spectra showed only $[Mn(bpy)(CO)_3H]$ formation, confirming past predictions that CO_2 binding to $[Mn(bpy)(CO)_3]^-$ is endergonic in the absence of a suitably strong acid.[39] Instead in weak acids, catalysis is thought to occur via the formation of $[Mn(bpy)(CO)_3(CO_2)]^{2-}$, which occurs only at potentials more negative than examined in our work.[39]

Past DFT and microkinetic simulations predicted that $[Mn(bpy)(OCOH)]$ and $[Mn(bpy(CO_2H)]^-$ would be the main intermediates observed under CO_2 when TFE and phenol were the acid sources at −1.7 and −2.0 V_{SCE}, respectively.[37] However, isotopic labeling experiments and DFT calculations of the Stark tuning rates of the ν(CO) modes of the CO_2 intermediate ruled out assignment to $[Mn(bpy)(OCOH)]$, and the VSFG bands at ∼1976 and 1600 cm^{-1}

https://doi.org/10.1021/acs.accounts.1c00692
Acc. Chem. Res. 2022, 55, 955−965

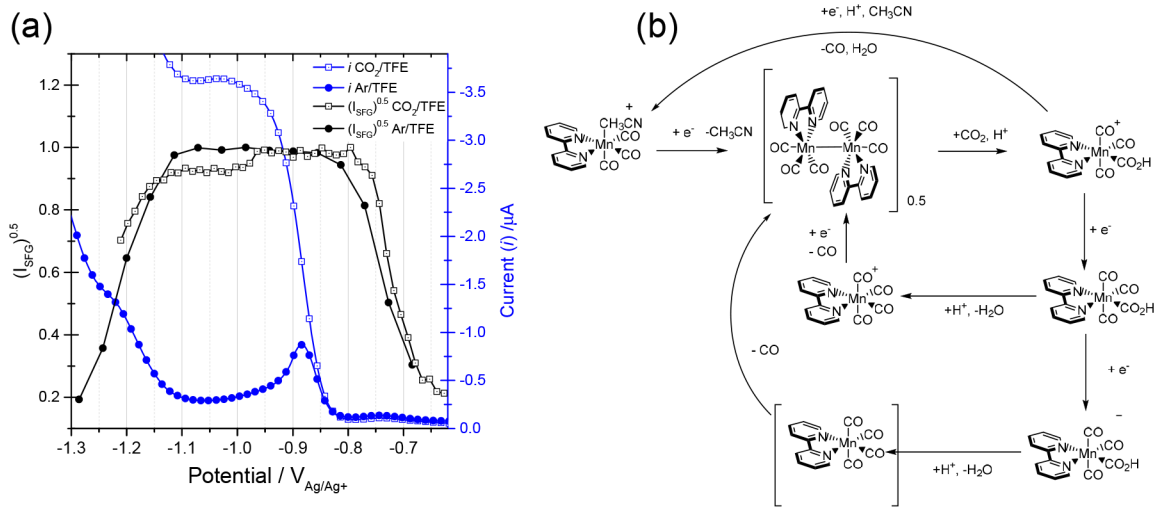

Figure 7. (a) Square root of VSFG intensity of a ν(CO) band of $[Mn_2(bpy)_2(CO)_6]$ under CO_2 and Ar gives a measure of the concentration of this species at the electrode as the potential is changed. The current recorded during the experiment is in blue. (b) Analysis of VSFG data leads to a new proposed pathway (bottom) for CO production via the reduction of $[Mn(bpy)(CO)_3(CO_2H)]$. Reproduced from ref 4 with permission from the PCCP Owner Societies.

were assigned to $[Mn(bpy)(CO)_4]^+$, a later intermediate in the catalytic cycle of the "protonation first" pathway.[3] The VSFG data did support the proposed potential dependent switching between a protonation first and reduction first pathway,[38,39] with an additional band at ~1875 cm^{-1} possibly being due to $[Mn(bpy)(CO_2H)]^-$. The availability of the lower-overpotential protonation first pathway catalysis had also been demonstrated to occur elsewhere in several studies with derivatives of the Mn complex,[52,53] and its accessibility offers a further reason for the typically lower overpotentials and increased activity for CO_2 reduction using this class of Mn complexes in the presence of stronger acids.[37,38]

With $[Mn(bpy)(CO)_3Br]$, a CO_2 reduction current is also observed at potentials positive of $[Mn_2(bpy)_2(CO)_6]$ reduction, demonstrating the presence of an additional low-overpotential pathway to produce CO. The catalytic studies outlined in section 2 show that this "dimer pathway" (Figure 1b) also retains high selectivity toward CO production even in water. The mechanism of catalysis via the dimer was first studied through a combination of pulsed-EPR and UV/vis spectroscopy,[54] where it was shown that in a 5% water/95% CH_3CN solution CO_2 purging led to loss of electrochemically generated dimer in the bulk electrolyte.[55] Further UV/vis and FTIR studies of immobilized Mn catalysts also explored the reactivity of the dimer complex in the presence of water and showed that it was decreased within seconds of the electrolyte being exposed to CO_2.[56,57] However, the behavior of the dimer using different acid sources had not been previously studied in detail and VSFG spectroscopy also offered a way to analyze the possible role of surface specific species in the "dimer mechanism".[4]

In a homodyne experiment, it can be approximated that VSFG signal intensities scale quadratically with the density of vibrational modes in the interface region.[41] Therefore, a plot of the square root of the VSFG intensities versus electrode potential provides a semiquantitative measure of the surface/double layer concentration of the species. VSFG experiments looking at the behavior of $[Mn_2(bpy)_2(CO)_6]$ in CH_3CN with a range of acids added showed that the dimer accumulated and reached a plateau concentration at −0.7 V_{Ag} (Figure 7a) in the presence of TFE.[4] Under Ar, the surface population of $[Mn_2(bpy)_2(CO)_6]$ remained constant regardless of the acid used (TFE, phenol, no acid) until reduction occurred, and this led to the formation of $[Mn(bpy)(CO)_3H]$. Identical behavior was observed under CO_2 in the absence of an added acid, with $[Mn_2(bpy)_2(CO)_6]$ persisting at the electrode surface prior to $[Mn(bpy)(CO)_3H]$ formation occurring, indicating that CO_2 is unable to interact with the dimer without a suitable Brønsted acid. In the presence of either TFE or phenol and CO_2 a notable decrease in the surface concentration of $[Mn_2(bpy)_2(CO)_6]$ occurred, 130 mV positive of the reduction potential of $[Mn_2(bpy)_2(CO)_6]$. The extent of decrease in the VSFG signal of $[Mn_2(bpy)_2(CO)_6]$ was greatest when the lowest pK_a acid (phenol) and CO_2 were used indicating that CO_2 interaction with the dimer to produce the previously[54] detected *mer* $Mn^{II}-CO_2H$ also occurs via a protonation-assisted CO_2 binding mechanism. Furthermore, by analysis of the onset of the catalytic current and from knowledge of the electrochemical stability of previously proposed intermediates, a new alternative pathway for CO evolution following *mer*-$Mn^{II}-CO_2H$ formation via the reduction of a *mer*-$Mn(bpy)(CO)_3(CO_2H)$ intermediate occurs prior to protonation and H_2O loss (Figure 7b), different from those previously put forward by Deronzier and Grills.[22,54]

4. CONCLUSIONS AND OUTLOOK

VSFG spectroscopy can follow the Mn electrocatalyst for CO_2 reduction while at the electrode surface, and our results complement the theoretical and other spectroscopic studies in the literature to provide important insights into the remarkable selectivity of this class of catalysts toward CO_2 reduction. The low levels of H_2 production are not due to a lack of H^+ binding when the active $[Mn(bpy)(CO)_3]^-$ catalyst is generated as previously postulated, as $[Mn(bpy)(CO)_3H]$ forms rapidly at the electrode surface in the absence of CO_2. Instead selectivity toward CO_2 in all catalytic pathways ("dimer pathway" species 2 and 11; "protonation first" species 3, 5, 6, 8, and 9, and "reduction first" species 3, 5, 6, 7, and 9, Figure 1b) arises by

https://doi.org/10.1021/acs.accounts.1c00692
Acc. Chem. Res. 2022, 55, 955−965

an unusual acid-promoted CO_2 binding mechanism, where acids with a lower pK_a actually lead to higher concentrations of CO_2 reduction intermediates. We believe that such an effect has been rarely reported within the large variety of known homogeneous CO_2 reduction catalysts. To date, our studies have focused on one particular class of catalysts and not in aqueous solvent, which may complicate direct comparisons, but we encourage future works to explore if similar proton-assisted CO_2 binding mechanisms are in wider operation among CO_2 reduction catalysts.

Recent technoeconomic analyses highlight the need to understand and discover new electrocatalysts that can reduce CO_2 selectively in water, in particular at low pH.[27] There are relatively few studies to date on the use of this class of catalysts in water, but from the emerging literature, it does appear that the proton-assisted CO_2 binding mechanisms seen in aprotic solvents may be facilitating the measured high levels of selectivity in aqueous electrolytes as well. While the long-term stability of these Mn catalysts is uncertain, especially under high current densities, initial catalysis studies are promising, and these Mn complexes serve as valuable models for future development of proton/acid tolerant CO_2 reduction catalysts.

AUTHOR INFORMATION

Corresponding Author

Alexander J. Cowan − *Stephenson Institute for Renewable Energy and the Department of Chemistry, University of Liverpool, Liverpool L69 7ZF, U.K.;* orcid.org/0000-0001-9032-3548; Email: acowan@liverpool.ac.uk

Authors

Bhavin Siritanaratkul − *Stephenson Institute for Renewable Energy and the Department of Chemistry, University of Liverpool, Liverpool L69 7ZF, U.K.;* orcid.org/0000-0003-0604-7670

Catherine Eagle − *Stephenson Institute for Renewable Energy and the Department of Chemistry, University of Liverpool, Liverpool L69 7ZF, U.K.*

Complete contact information is available at: https://pubs.acs.org/10.1021/acs.accounts.1c00692

Notes

The authors declare no competing financial interest.

Biographies

Bhavin Siritanaratkul received his D.Phil. in Chemistry from the University of Oxford under the supervision of Fraser A. Armstrong, where he worked on the electrochemistry of enzymes for nicotinamide cofactor regeneration. His prior research experience includes solar water splitting and heterogeneous catalysis for methane conversion. He is currently a postdoctoral researcher with Alex Cowan at the University of Liverpool, working on electrochemical CO_2 reduction.

Catherine Eagle obtained her Masters in Science from Imperial College London (2020) under the supervision of Dr. Rob Davies. Following this, she moved to the University of Liverpool to join Prof. Alex Cowan's research group as a Ph.D. student to study carbon dioxide utilization by selective reduction of impure and low concentration carbon dioxide streams using molecular catalysts.

Alex Cowan is a Professor of Chemistry at the University of Liverpool where he leads an interdisciplinary team who are developing new catalysts and materials for the production of sustainable fuels and studying their mechanisms. A particular interest of the group is the electrocatalytic reduction of carbon dioxide into useful molecules such as carbon monoxide and the in situ studies of these electrocatalysts.

ACKNOWLEDGMENTS

A.C. and B.S. acknowledge UKRI-EPSRC (EP/V011863/1) for financial support. C.E. acknowledges NSG Pilkington for support of the Ph.D. studentship. The authors also thank both present and past colleagues for their contributions to the science described in this Account.

REFERENCES

(1) Walsh, J. J.; Neri, G.; Smith, C. L.; Cowan, A. J. Electrocatalytic CO2 reduction with a membrane supported manganese catalyst in aqueous solution. *Chem. Commun.* **2014**, *50* (84), 12698−12701.

(2) Walsh, J. J.; Neri, G.; Smith, C. L.; Cowan, A. J. Water-Soluble Manganese Complex for Selective Electrocatalytic CO2 Reduction to CO. *Organometallics* **2019**, *38* (6), 1224−1229.

(3) Neri, G.; Walsh, J. J.; Teobaldi, G.; Donaldson, P. M.; Cowan, A. J. Detection of catalytic intermediates at an electrode surface during carbon dioxide reduction by an earth-abundant catalyst. *Nature Catalysis* **2018**, *1* (12), 952−959.

(4) Neri, G.; Donaldson, P. M.; Cowan, A. J. In situ study of the low overpotential "dimer pathway" for electrocatalytic carbon dioxide reduction by manganese carbonyl complexes. *Phys. Chem. Chem. Phys.* **2019**, *21* (14), 7389−7397.

(5) Kibria, M. G.; Edwards, J. P.; Gabardo, C. M.; Dinh, C.-T.; Seifitokaldani, A.; Sinton, D.; Sargent, E. H. Electrochemical CO2 Reduction into Chemical Feedstocks: From Mechanistic Electrocatalysis Models to System Design. *Adv. Mater.* **2019**, *31* (31), 1807166.

(6) Birdja, Y. Y.; Pérez-Gallent, E.; Figueiredo, M. C.; Göttle, A. J.; Calle-Vallejo, F.; Koper, M. T. M. Advances and challenges in understanding the electrocatalytic conversion of carbon dioxide to fuels. *Nature Energy* **2019**, *4* (9), 732−745.

(7) Francke, R.; Schille, B.; Roemelt, M. Homogeneously Catalyzed Electroreduction of Carbon Dioxide-Methods, Mechanisms, and Catalysts. *Chem. Rev.* **2018**, *118* (9), 4631−4701.

(8) Hori, Y. Electrochemical CO2 Reduction on Metal Electrodes. In *Modern Aspects of Electrochemistry*; Vayenas, C. G., White, R. E., Gamboa-Aldeco, M. E., Eds.; Springer New York: New York, NY, 2008; pp 89−189.

(9) García de Arquer, F. P.; Dinh, C.-T.; Ozden, A.; Wicks, J.; McCallum, C.; Kirmani, A. R.; Nam, D.-H.; Gabardo, C.; Seifitokaldani, A.; Wang, X.; Li, Y. C.; Li, F.; Edwards, J.; Richter, L. J.; Thorpe, S. J.; Sinton, D.; Sargent, E. H. CO2 electrolysis to multicarbon products at activities greater than 1 A cm-2. *Science* **2020**, *367* (6478), 661−666.

(10) Li, C.; Xiong, H.; He, M.; Xu, B.; Lu, Q. Oxyhydroxide Species Enhances CO2 Electroreduction to CO on Ag via Coelectrolysis with O2. *ACS Catal.* **2021**, *11* (19), 12029−12037.

(11) Xu, Y.; Edwards, J. P.; Zhong, J.; O'Brien, C. P.; Gabardo, C. M.; McCallum, C.; Li, J.; Dinh, C.-T.; Sargent, E. H.; Sinton, D. Oxygen-tolerant electroproduction of C2 products from simulated flue gas. *Energy Environ. Sci.* **2020**, *13* (2), 554−561.

(12) Jiang, C.; Nichols, A. W.; Machan, C. W. A look at periodic trends in d-block molecular electrocatalysts for CO2 reduction. *Dalton Trans* **2019**, *48* (26), 9454−9468.

(13) Kinzel, N. W.; Werle, C.; Leitner, W. Transition Metal Complexes as Catalysts for the Electroconversion of CO2: An Organometallic Perspective. *Angew. Chem., Int. Ed. Engl.* **2021**, *60* (21), 11628−11686.

(14) Liu, D.-C.; Zhong, D.-C.; Lu, T.-B. Non-noble metal-based molecular complexes for CO2 reduction: From the ligand design perspective. *EnergyChem.* **2020**, *2* (3), 100034.

(15) Amanullah, S.; Saha, P.; Nayek, A.; Ahmed, M. E.; Dey, A. Biochemical and artificial pathways for the reduction of carbon dioxide, nitrite and the competing proton reduction: effect of 2(nd) sphere interactions in catalysis. *Chem. Soc. Rev.* **2021**, *50* (6), 3755−3823.
(16) Hawecker, J.; Lehn, J.-M.; Ziessel, R. Electrocatalytic reduction of carbon dioxide mediated by Re(bipy)(CO)3Cl (bipy = 2,2′-bipyridine). *J. Chem. Soc., Chem. Commun.* **1984**, No. 6, 328−330.
(17) Hawecker, J.; Lehn, J.-M.; Ziessel, R. Efficient photochemical reduction of CO2 to CO by visible light irradiation of systems containing Re(bipy)(CO)3X or Ru(bipy)32+-Co2+ combinations as homogeneous catalysts. *J. Chem. Soc., Chem. Commun.* **1983**, No. 9, 536−538.
(18) Yaroshevsky, A. A. Abundances of chemical elements in the Earth's crust. *Geochemistry International* **2006**, *44* (1), 48−55.
(19) Johnson, F. P. A.; George, M. W.; Hartl, F.; Turner, J. J. Electrocatalytic Reduction of CO2 Using the Complexes [Re(bpy)-(CO)3L]n (n = + 1, L = P(OEt)3, CH3CN; n = 0, L = Cl-, Otf-; bpy = 2,2‘-Bipyridine; Otf- = CF3SO3) as Catalyst Precursors: Infrared Spectroelectrochemical Investigation. *Organometallics* **1996**, *15* (15), 3374−3387.
(20) Bourrez, M.; Molton, F.; Chardon-Noblat, S.; Deronzier, A. [Mn(bipyridyl)(CO)3Br]: an abundant metal carbonyl complex as efficient electrocatalyst for CO2 reduction. *Angew. Chem., Int. Ed. Engl.* **2011**, *50* (42), 9903−6.
(21) Barrett, J. A.; Miller, C. J.; Kubiak, C. P. Electrochemical Reduction of CO2 Using Group VII Metal Catalysts. *Trends in Chemistry* **2021**, *3* (3), 176−187.
(22) Grills, D. C.; Ertem, M. Z.; McKinnon, M.; Ngo, K. T.; Rochford, J. Mechanistic aspects of CO2 reduction catalysis with manganese-based molecular catalysts. *Coord. Chem. Rev.* **2018**, *374*, 173−217.
(23) Sinopoli, A.; La Porte, N. T.; Martinez, J. F.; Wasielewski, M. R.; Sohail, M. Manganese carbonyl complexes for CO2 reduction. *Coord. Chem. Rev.* **2018**, *365*, 60−74.
(24) Stanbury, M.; Compain, J.-D.; Chardon-Noblat, S. Electro and photoreduction of CO2 driven by manganese-carbonyl molecular catalysts. *Coord. Chem. Rev.* **2018**, *361*, 120−137.
(25) Smieja, J. M.; Sampson, M. D.; Grice, K. A.; Benson, E. E.; Froehlich, J. D.; Kubiak, C. P. Manganese as a Substitute for Rhenium in CO2 Reduction Catalysts: The Importance of Acids. *Inorg. Chem.* **2013**, *52* (5), 2484−2491.
(26) Li, J.; Kornienko, N. Electrocatalytic carbon dioxide reduction in acid. *Chem. Catalysis* **2022**, *2* (1), 29−38.
(27) Rabinowitz, J. A.; Kanan, M. W. The future of low-temperature carbon dioxide electrolysis depends on solving one basic problem. *Nat. Commun.* **2020**, *11* (1), 5231.
(28) Reuillard, B.; Ly, K. H.; Rosser, T. E.; Kuehnel, M. F.; Zebger, I.; Reisner, E. Tuning Product Selectivity for Aqueous CO2 Reduction with a Mn(bipyridine)-pyrene Catalyst Immobilized on a Carbon Nanotube Electrode. *J. Am. Chem. Soc.* **2017**, *139* (41), 14425−14435.
(29) Yoshida, T.; Tsutsumida, K.; Teratani, S.; Yasufuku, K.; Kaneko, M. Electrocatalytic reduction of CO2 in water by [Re(bpy)(CO)3Br] and [Re(terpy)(CO)3Br] complexes incorporated into coated nafion membrane (bpy = 2,2′-bipyridine; terpy = 2,2′;6′,2″-terpyridine). *J. Chem. Soc., Chem. Commun.* **1993**, No. 7, 631−633.
(30) Walsh, J. J.; Smith, C. L.; Neri, G.; Whitehead, G. F. S.; Robertson, C. M.; Cowan, A. J. Improving the efficiency of electrochemical CO2 reduction using immobilized manganese complexes. *Faraday Discuss.* **2015**, *183* (0), 147−160.
(31) Sato, S.; Saita, K.; Sekizawa, K.; Maeda, S.; Morikawa, T. Low-Energy Electrocatalytic CO2 Reduction in Water over Mn-Complex Catalyst Electrode Aided by a Nanocarbon Support and K+ Cations. *ACS Catal.* **2018**, *8* (5), 4452−4458.
(32) Rotundo, L.; Filippi, J.; Gobetto, R.; Miller, H. A.; Rocca, R.; Nervi, C.; Vizza, F. Electrochemical CO2 reduction in water at carbon cloth electrodes functionalized with a fac-Mn(apbpy)(CO)3Br complex. *Chem. Commun.* **2019**, *55* (6), 775−777.
(33) Filippi, J.; Rotundo, L.; Gobetto, R.; Miller, H. A.; Nervi, C.; Lavacchi, A.; Vizza, F. Turning manganese into gold: Efficient electrochemical CO2 reduction by a fac-Mn(apbpy)(CO)3Br complex in a gas-liquid interface flow cell. *Chem. Eng. J.* **2021**, *416*, 129050.
(34) Smith, C. L.; Clowes, R.; Sprick, R. S.; Cooper, A. I.; Cowan, A. J. Metal-organic conjugated microporous polymer containing a carbon dioxide reduction electrocatalyst. *Sustainable Energy & Fuels* **2019**, *3* (11), 2990−2994.
(35) Dubed Bandomo, G. C.; Mondal, S. S.; Franco, F.; Bucci, A.; Martin-Diaconescu, V.; Ortuño, M. A.; van Langevelde, P. H.; Shafir, A.; López, N.; Lloret-Fillol, J. Mechanically Constrained Catalytic Mn(CO)3Br Single Sites in a Two-Dimensional Covalent Organic Framework for CO2 Electroreduction in H2O. *ACS Catal.* **2021**, *11* (12), 7210−7222.
(36) Nakada, A.; Ishitani, O. Selective Electrocatalysis of a Water-Soluble Rhenium(I) Complex for CO2 Reduction Using Water As an Electron Donor. *ACS Catal.* **2018**, *8* (1), 354−363.
(37) Riplinger, C.; Carter, E. A. Influence of Weak Brønsted Acids on Electrocatalytic CO2 Reduction by Manganese and Rhenium Bipyridine Catalysts. *ACS Catal.* **2015**, *5* (2), 900−908.
(38) Riplinger, C.; Sampson, M. D.; Ritzmann, A. M.; Kubiak, C. P.; Carter, E. A. Mechanistic contrasts between manganese and rhenium bipyridine electrocatalysts for the reduction of carbon dioxide. *J. Am. Chem. Soc.* **2014**, *136* (46), 16285−98.
(39) Lam, Y. C.; Nielsen, R. J.; Gray, H. B.; Goddard, W. A. A Mn Bipyrimidine Catalyst Predicted To Reduce CO2 at Lower Overpotential. *ACS Catal.* **2015**, *5* (4), 2521−2528.
(40) Neri, G.; Donaldson, P. M.; Cowan, A. J. The Role of Electrode-Catalyst Interactions in Enabling Efficient CO2 Reduction with Mo(bpy)(CO)4 As Revealed by Vibrational Sum-Frequency Generation Spectroscopy. *J. Am. Chem. Soc.* **2017**, *139* (39), 13791−13797.
(41) Gardner, A. M.; Saeed, K. H.; Cowan, A. J. Vibrational sum-frequency generation spectroscopy of electrode surfaces: studying the mechanisms of sustainable fuel generation and utilisation. *Phys. Chem. Chem. Phys.* **2019**, *21* (23), 12067−12086.
(42) Lambert, A. G.; Davies, P. B.; Neivandt, D. J. Implementing the Theory of Sum Frequency Generation Vibrational Spectroscopy: A Tutorial Review. *Appl. Spectrosc. Rev.* **2005**, *40* (2), 103−145.
(43) Rey, N. G.; Dlott, D. D. Studies of electrochemical interfaces by broadband sum frequency generation. *J. Electroanal. Chem.* **2017**, *800*, 114−125.
(44) Ohno, P. E.; Wang, H.-f.; Geiger, F. M. Second-order spectral lineshapes from charged interfaces. *Nat. Commun.* **2017**, *8* (1), 1032.
(45) Grills, D. C.; Farrington, J. A.; Layne, B. H.; Lymar, S. V.; Mello, B. A.; Preses, J. M.; Wishart, J. F. Mechanism of the formation of a Mn-based CO2 reduction catalyst revealed by pulse radiolysis with time-resolved infrared detection. *J. Am. Chem. Soc.* **2014**, *136* (15), 5563−6.
(46) Franco, F.; Cometto, C.; Nencini, L.; Barolo, C.; Sordello, F.; Minero, C.; Fiedler, J.; Robert, M.; Gobetto, R.; Nervi, C. Local Proton Source in Electrocatalytic CO2 Reduction with [Mn(bpy-R)(CO)3 Br] Complexes. *Chemistry* **2017**, *23* (20), 4782−4793.
(47) Scheiring, T.; Kaim, W.; Fiedler, J. Geometrical and electronic structures of the acetyl complex Re(bpy)(CO)3(COCH3) and of [M(bpy)(CO)4](OTf), M = Mn,Re. *J. Organomet. Chem.* **2000**, *598* (1), 136−141.
(48) Machan, C. W.; Sampson, M. D.; Chabolla, S. A.; Dang, T.; Kubiak, C. P. Developing a Mechanistic Understanding of Molecular Electrocatalysts for CO2 Reduction using Infrared Spectroelectrochemistry. *Organometallics* **2014**, *33* (18), 4550−4559.
(49) Neri, G.; Donaldson, P. M.; Cowan, A. J. *Vibrational Sum Frequency Generation (VSFG) Spectroscopy of Electrocatalytic Mechanisms*; CLF Annual Report, 2017.
(50) Sampson, M. D.; Nguyen, A. D.; Grice, K. A.; Moore, C. E.; Rheingold, A. L.; Kubiak, C. P. Manganese Catalysts with Bulky

Bipyridine Ligands for the Electrocatalytic Reduction of Carbon Dioxide: Eliminating Dimerization and Altering Catalysis. *J. Am. Chem. Soc.* **2014**, *136* (14), 5460−5471.
(51) Schultz, Z. D.; Shaw, S. K.; Gewirth, A. A. Potential Dependent Organization of Water at the Electrified Metal-Liquid Interface. *J. Am. Chem. Soc.* **2005**, *127* (45), 15916−15922.
(52) Ngo, K. T.; McKinnon, M.; Mahanti, B.; Narayanan, R.; Grills, D. C.; Ertem, M. Z.; Rochford, J. Turning on the Protonation-First Pathway for Electrocatalytic CO2 Reduction by Manganese Bipyridyl Tricarbonyl Complexes. *J. Am. Chem. Soc.* **2017**, *139* (7), 2604−2618.
(53) Yang, Y.; Ertem, M. Z.; Duan, L. An amide-based second coordination sphere promotes the dimer pathway of Mn-catalyzed CO2-to-CO reduction at low overpotential. *Chemical Science* **2021**, *12* (13), 4779−4788.
(54) Bourrez, M.; Orio, M.; Molton, F.; Vezin, H.; Duboc, C.; Deronzier, A.; Chardon-Noblat, S. Pulsed-EPR evidence of a manganese(II) hydroxycarbonyl intermediate in the electrocatalytic reduction of carbon dioxide by a manganese bipyridyl derivative. *Angew. Chem., Int. Ed. Engl.* **2014**, *53* (1), 240−3.
(55) Hayashi, Y.; Kita, S.; Brunschwig, B. S.; Fujita, E. Involvement of a Binuclear Species with the Re-C(O)O-Re Moiety in CO2 Reduction Catalyzed by Tricarbonyl Rhenium(I) Complexes with Diimine Ligands: Strikingly Slow Formation of the Re-Re and Re-C(O)O-Re Species from Re(dmb)(CO)3S (dmb = 4,4′-Dimethyl-2,2′-bipyridine, S = Solvent). *J. Am. Chem. Soc.* **2003**, *125* (39), 11976−11987.
(56) Rosser, T. E.; Windle, C. D.; Reisner, E. Electrocatalytic and Solar-Driven CO2 Reduction to CO with a Molecular Manganese Catalyst Immobilized on Mesoporous TiO2. *Angew. Chem., Int. Ed. Engl.* **2016**, *55* (26), 7388−92.
(57) Walsh, J. J.; Forster, M.; Smith, C. L.; Neri, G.; Potter, R. J.; Cowan, A. J. Directing the mechanism of CO2 reduction by a Mn catalyst through surface immobilization. *Phys. Chem. Chem. Phys.* **2018**, *20* (10), 6811−6816.

https://doi.org/10.1021/acs.accounts.1c00692
Acc. Chem. Res. 2022, 55, 955−965